The 4th International Symposium on More Electric Aircraft Technology (MEA 2017)

8–9 November 2017

Model predictive control for reduced matrix converter with transformer DC magnetic bias suppression

Wei-Zhang Song[1,2], Jiang Liu[1], Da-Qing Gao[3], Feng-Jun Wu[3], You-Yun Wang[2]

[1]*Department of Electrical Engineering, Xi'an University of Technology, Xi'an, Shaanxi, People's Republic of China*
[2]*State Key Laboratory of Large Electric Drive System and Equipment Technology, Tianshui, Gansu, People's Republic of China*
[3]*Institute of Modern Physics, Lan zhou, Gansu, People's Republic of China*
E-mail: lj15667083657@126.com

Published in *The Journal of Engineering*; Received on 10th January 2018; Accepted on 17th January 2018

Abstract: This study presents a model predictive control (MPC) considering transformer DC magnetic bias for a reduced matrix converter (RMC). The control scheme selects the switching state that minimises the error in the output current and input instantaneous reactive according to their reference values; furthermore, the pulse sequence in MPC has been re-distributed to suppress the DC magnetic bias in transformer for RMC. MPC also presents stronger immunity to the influence of abnormal input voltage than bipolar space vector modulation strategy. Moreover, the simple performance comparison between RMC and pulse-width modulated rectifier + dual active bridge was provided. The feasibility and validity of the proposed control scheme in an RMC has been verified by simulation results.

1 Introduction

Matrix converter (MC) offers an 'all silicon solution' for direct power converter; reduced matrix converter (RMC) originating from MC is one new type topology in power electronic converters in the past decade. RMC has all good advantages of MC, but avoids its some drawbacks, such as electrical isolation between the input power and load, and low-voltage transfer ratio. RMC has attracted plenty of attention and great potential application in the field of power electronics such as switching power supply, wind power generation, high-voltage direct current (DC) transmission, and so on [1, 2].

The main control algorithm of RMC is bipolar space vector modulation strategy (B-C-SVM), RMC controlled by this strategy outputs high-frequency positive and negative pulse voltage in the DC-link. However, the input and output currents are easily disturbed since this strategy is equivalent to an open-loop control method [3–5]. Model predictive control (MPC) has been reported as a promising control scheme due to its advantages over traditional linear controllers, such as fast dynamic responses, easy inclusion of non-linearities and system constraints, strong disturbance resistibility, and the fact that no modulators are needed [6].

Recently, it has been successfully applied to the control of inverter, pulse-width modulated (PWM) rectifier, and MC topology [7–9]. As a new topology in RMC, the current research work in RMC is mainly focused on modulation strategy, efficiency, and performance comparison [1–5]. The MPC is not applied to RMC according to the existing literatures.

This paper firstly introduces MPC to RMC topology; furthermore, the MPC has been improved in terms of pulse sequence distributing to solve the problem of DC magnetic bias in transformer for this topology. The simple comparison between RMC and the other topology with the same performance named PRDAB (PWM rectifier + dual active bridge) was provided.

2 Methodology

2.1 Topological structure of RMC

The conventional converter for three-phase AC to an alternated DC consists of PRDAB shown in Fig. 1*a*. The schematic diagram of power flow for PRDAB is shown in Fig. 1*b*.

The topology of RMC is shown in Fig. 2*a*; it consists of five parts: input power, input filter, RMC rectifier stage, high-frequency transformer, controlled rectifier bridge, and load, without any bulky capacitor in DC-link [5]. The RMC rectifier stage realises power conversion from the three-phase AC voltage to the high-frequency pulse voltage. The high-frequency transformer plays a role of electrical isolation and voltage regulation. The controlled rectifier bridge realises power conversion from the high-frequency pulse voltage to DC voltage.

Comparing with the two topologies, the DC-link energy storage element of PRDAB has a relatively large physical volume compared with the total converter volume [10]. However, the power unit for switch number is only two differences (14 for PRDAB, 16 for RMC); thus, the power density of RMC is higher than PRDAB. How long time a system work depend on lifetime of devices. Assuming that the lifetime of the switches in the two topologies is the same, the lifetime of energy storage capacitor is short, which is the key factor of system lifetime [11]; thus, the lifetime of RMC without DC-link capacitor is longer than PRDAB. The value of input inductance in PRDAB is larger than the value of input inductor in RMC [12]. The large filter inductance will affect the system conversion efficiency. There are zero vectors with making a soft-switch function in the modulation strategy of RMC. Furthermore, seen from Figs. 1*b* and 2*b*, the stage of power converter in RMC with two stage is less than converter stage in PRDAB with three stage; thus, the efficiency of RMC is higher than PRDAB. The results of the comparative evaluation are compiled in Table 1.

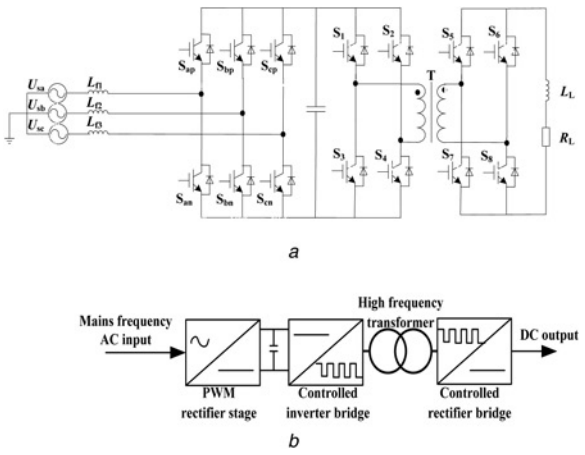

Fig. 1 *PWM rectifier + dual active bridge*
a The topology of PRDAB
b Schematic diagram of PRDAB

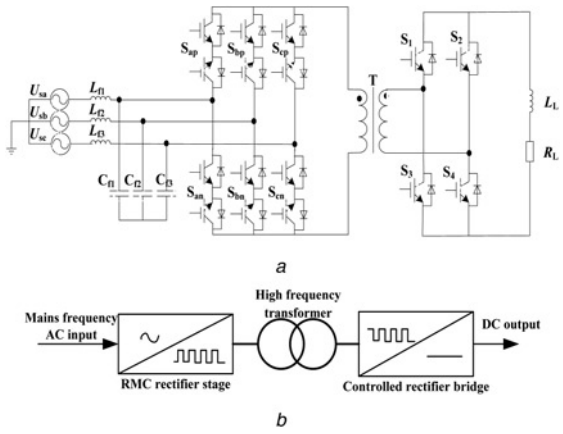

Fig. 2 *Reduced matrix converter*
a The topology of RMC
b Schematic diagram of RMC

Table 1 Comparisons of two topologies

	PRBDAB	RMC
DC-link energy storage capacitor	no	yes
value of input filter inductor	large	small
high-frequency transformers	yes	yes
number of switching tubes	14	16
bidirectional flow of energy	yes	yes
power density	normal	high
soft-switch	no	yes
efficiency	normal	high
lifetime	normal	long

2.2 MPC for RMC with eliminating transformer bias magnet

MPC with transformer DC magnetic bias suppression in an RMC is based on the mathematical model and differential constraints of the system. Using the known amount of states, the input and output currents can be predicted by combining all possible switching states in one sampling period. According to the quality function, the optimal switching state has been selected to make the target variable of the next sampling time be forced to follow the reference value [8, 9, 13]. The block diagram of the system control is shown in Fig. 3.

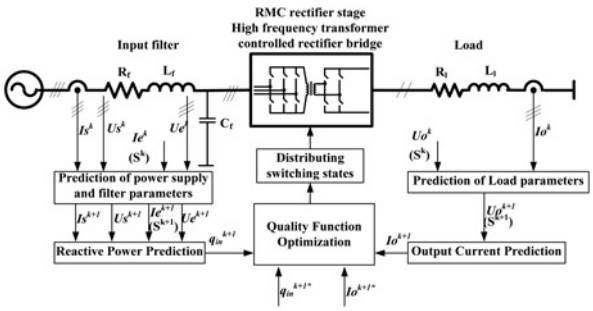

Fig. 3 *Block diagram of system control*

Also, the main steps of this control method are listed as follows:

(i) establishing mathematical model of RMC;
(ii) building all possible switching states;
(iii) calculation of predicted values;
(iv) establishing the quality function;
(v) distributing switching states with transformer DC magnetic bias suppression.

2.2.1 Establishing mathematical model of RMC: The input filter circuit in RMC is shown in Fig. 4. Its mathematical model can be expressed as follows:

$$L_{\mathrm{f}}\frac{\mathrm{d}\boldsymbol{i}_{\mathrm{s}}}{\mathrm{d}t}=\boldsymbol{u}_{\mathrm{s}}-\boldsymbol{u}_{\mathrm{e}}-R_{\mathrm{f}}\cdot\boldsymbol{i}_{\mathrm{s}} \tag{1}$$

$$C_{\mathrm{f}}\frac{\mathrm{d}\boldsymbol{u}_{e}}{\mathrm{d}t}=\boldsymbol{i}_{\mathrm{s}}-\boldsymbol{i}_{e} \tag{2}$$

where u_{s} and i_{s} are the source-side voltage and current, respectively. u_e and i_e are the input voltage and current of RMC rectifier stage, respectively, R_{f}, L_{f}, and C_{f} are equivalent resistance, inductance, and capacitor of the input filter.

The RMC rectifier stage circuit shown in Fig. 5 can be represented using:

$$u_{\mathrm{dc}}=[\,S_{ap}-S_{an}\quad S_{bp}-S_{bn}\quad S_{cp}-S_{cn}\,]\cdot\boldsymbol{u}_{e} \tag{3}$$

$$\boldsymbol{i}_{e}=\begin{bmatrix}S_{ap}-S_{an}\\ S_{bp}-S_{bn}\\ S_{cp}-S_{cn}\end{bmatrix}\cdot i_{\mathrm{dc}} \tag{4}$$

where u_{dc} and i_{dc} are voltage and current of the high-frequency transformer, respectively, and S_{ap}, S_{bp}, S_{cp}, S_{an}, S_{bn}, and S_{cn} the switching states of RMC rectifier stage.

The high-frequency transformer circuit shown in Fig. 6 can be expressed as follows:

$$u_1=n{*}u_{\mathrm{dc}} \tag{5}$$

$$i_{\mathrm{dc}}=n{*}i_1 \tag{6}$$

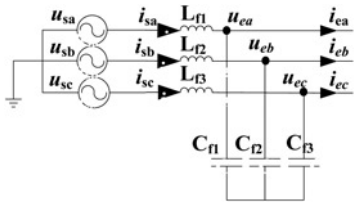

Fig. 4 *Input filter circuit*

doi: 10.1049/joe.2018.0036

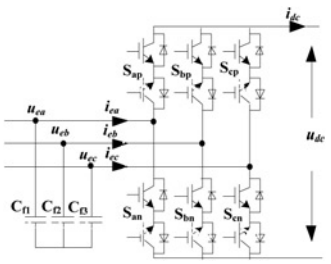

Fig. 5 *RMC rectifier stage circuit*

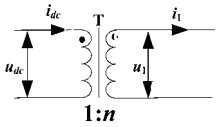

Fig. 6 *High-frequency transformer circuit*

where n is the transformer ratio, u_1 and i_1 are the side voltage and current of the high-frequency transformer, respectively.

The controlled rectifier bridge circuit shown in Fig. 7 can be expressed as follows:

$$u_0 = u_1(S_1 - S_3) \tag{7}$$

$$i_0 = i_1(S_1 - S_3) \tag{8}$$

where S_1 and S_3 are switching states of the controlled rectifier bridge, u_0 and i_0 the output voltage and current, respectively.

Similarly, mathematical model of the load voltage and current (Fig. 8) can be described by (9), where R_l and L_l are the resistance and inductance of the load, respectively

$$L_l \frac{\mathrm{d}\boldsymbol{i}_0}{\mathrm{d}t} = \boldsymbol{u}_0 - R_l \cdot \boldsymbol{i}_0 \tag{9}$$

2.2.2 Switching states and their combinations: Since in any MC topology, the input phases cannot be short circuit as well as the load cannot be in an open circuit due to inductive nature. There are nine switching states in three-phase rectifier bridge of RMC. In order to improve the voltage transfer ratio, the three zero vectors are removed.

Table 2 shows all the possible switching states generated by the RMC rectifier stage. Similarly, Table 3 shows all the possible switching states generated by the controlled rectifier bridge. Owing to fewer conversion progressions, RMC has a total of 12 switch combinations.

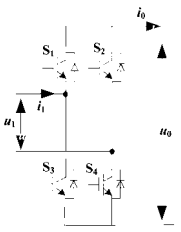

Fig. 7 *Controlled rectifier bridge circuit*

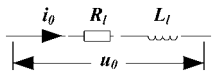

Fig. 8 *Load circuit*

Table 2 Switching states of RMC rectifier stage

Pulse sequence	U_{dc}	S_{ap}	S_{an}	S_{bp}	S_{bn}	S_{cp}	S_{cn}
V_1	U_{ab}	1	0	0	1	0	0
V_2	U_{ac}	1	0	0	0	0	1
V_3	U_{bc}	0	0	1	0	0	1
V_4	U_{ba}	0	1	1	0	0	0
V_5	U_{ca}	0	1	0	0	1	0
V_6	U_{cb}	0	0	0	1	1	0
V_7	U_{aa}	1	1	0	0	0	0
V_8	U_{bb}	0	0	1	1	0	0
V_9	U_{cc}	0	0	0	0	1	1

Table 3 Switching states of the controlled rectifier bridge

	S_1	S_2	S_3	S_4	i_{o}
1	1	0	0	1	i_1
2	0	1	1	0	$-i_1$

2.2.3 Calculation of predicted values: The prediction of the input currents of source-side and voltages of RMC rectifier stage are computed from a first-order difference equation. They can be calculated by representing (1) and (2) by a state-space system with state variables $i_{\mathrm{s}}^{(k+1)}$ and $u_e^{(k+1)}$

$$\begin{bmatrix} \boldsymbol{u}_e^{k+1} \\ \boldsymbol{i}_{\mathrm{s}}^{k+1} \end{bmatrix} = C \begin{bmatrix} \boldsymbol{u}_e^{k} \\ \boldsymbol{i}_{\mathrm{s}}^{k} \end{bmatrix} + D \begin{bmatrix} \boldsymbol{u}_{\mathrm{s}}^{k} \\ \boldsymbol{i}_e^{k} \end{bmatrix} \tag{10}$$

where

$$C = \begin{bmatrix} C_{11} & C_{12} \\ C_{21} & C_{22} \end{bmatrix} = \mathrm{e}^{ATs} \tag{11}$$

$$D = \begin{bmatrix} D_{11} & D_{12} \\ D_{21} & D_{22} \end{bmatrix} = A^{-1}(C - I_{2*2})B \tag{12}$$

$$A = \begin{bmatrix} 0 & \dfrac{1}{C_{\mathrm{f}}} \\ -\dfrac{1}{L_{\mathrm{f}}} & -\dfrac{R_{\mathrm{f}}}{L_{\mathrm{f}}} \end{bmatrix}, \quad B = \begin{bmatrix} 0 & -\dfrac{1}{C_{\mathrm{f}}} \\ \dfrac{1}{L_{\mathrm{f}}} & 0 \end{bmatrix} \tag{13}$$

Similarly, the discrete output current equation can be obtained as follows:

$$\boldsymbol{i}_{\mathrm{o}}^{(k+1)} = \frac{T_{\mathrm{s}}}{L_1}\boldsymbol{u}_o^{(k)} + \left(1 - \frac{R_1 T_{\mathrm{s}}}{L_1}\right)\boldsymbol{i}_{\mathrm{o}}^{(k)} \tag{14}$$

2.2.4 Establishing the quality function: The control objectives of the method that has been proposed are input reactive power and output currents. Therefore, two main conditions must be met as follows [14, 15].

(i) The reactive power in source-side closes to zero.
(ii) The output currents follow the reference value with high accuracy.

The first condition is accomplished by minimising the predicted instantaneous reactive power:

$$\Delta q_{\text{in}}^{(k+1)} = \left|0 - \left(U_{s\alpha}^{(k+1)} I_{s\beta}^{(k+1)} - U_{s\beta}^{(k+1)} I_{s\alpha}^{(k+1)}\right)\right| \tag{15}$$

where $U_{sa}^{(k+1)}$, $U_{s\beta}^{(k+1)}$, $i_{sa}^{(k+1)}$, and $i_{s\beta}^{(k+1)}$ are the source-side voltage and current at the next sampling time in $a\beta$ coordinates, respectively.

The second condition can be achieved through minimising the output currents between the prediction and reference as follows:

$$\Delta I_0^{(k+1)} = \left|I_0^* - I_0^{(k+1)}\right| \tag{16}$$

where I_0^* is the reference value and $I_0^{(k+1)}$ the output current in the next sampling time.

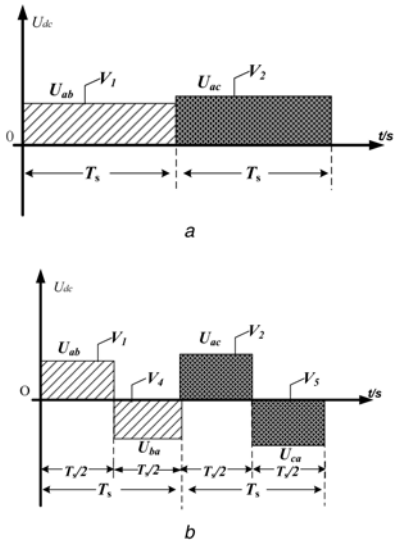

Fig. 9 *Diagram of RMC rectifier stage output voltage sequence*
a Without bias suppression
b With bias suppression

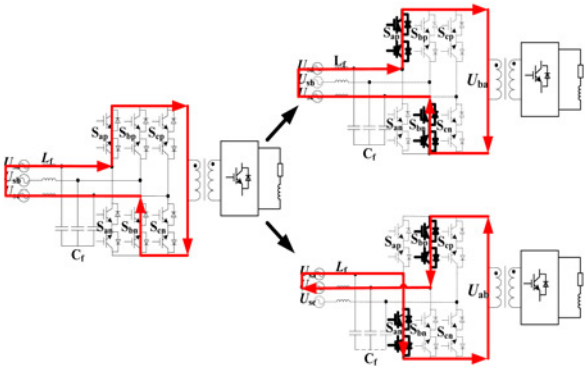

Fig. 10 *Equivalent circuit under opposite output voltage vector*

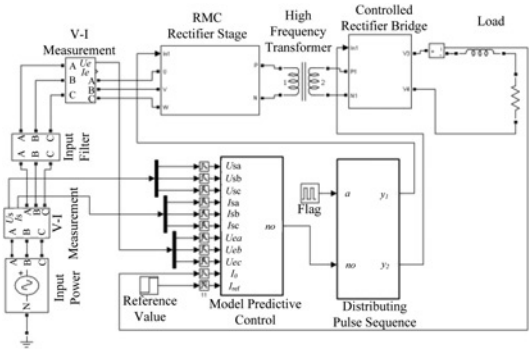

Fig. 11 *Simulink model of RMC*

Table 4 Simulation parameter

input filters	$R_f = 5\ \Omega$; $L_f = 1.4$ mH; $C_f = 21\ \mu$F
load	$R_l = 1\ \Omega$; $L_l = 10$ mH
power supply	311 V/50 Hz
λ	0.005
current reference value	$t < 0.2$ s:25 A $t > 0.2$ s:50 A
switching frequency	10 kHz

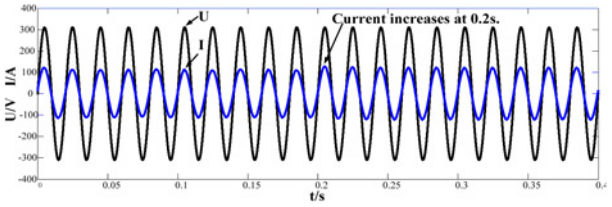

Fig. 12 *Voltage and current of source-side*

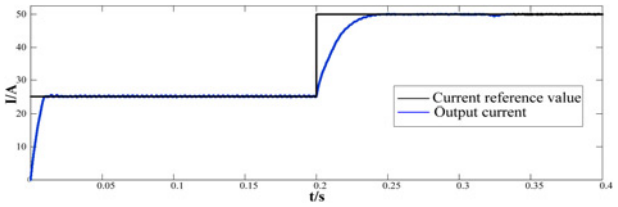

Fig. 13 *Output current and current reference value*

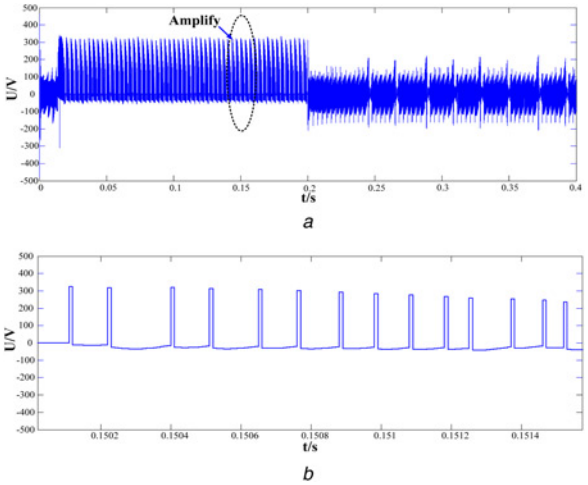

Fig. 14 *Voltage of transformer primary side*
a Voltage of transformer primary side without transformer DC magnetic bias suppression
b Local amplification of voltage

doi: 10.1049/joe.2018.0036

Two requirements can be merged into a single quality function as following, which is evaluated at every switching state:

$$g^{(k+1)} = \Delta I_0^{(k+1)} + \lambda \Delta q_{\text{in}}^{(k+1)} \tag{17}$$

where λ is a weighting factor, which is used to determine the importance or priority between the output current and power factor. The weighting factor is selected based on the evolution method in terms of the error of input reactive power and output current tracking [16].

It is obvious that the control objectives in the quality function are the output current and the reactive power on the grid side. We all know that MPC has the characteristics of real-time receding horizon optimisation. According to this characteristics of MPC, the system can also guarantee the input unit power factor and the output follow the reference even though in the operating condition

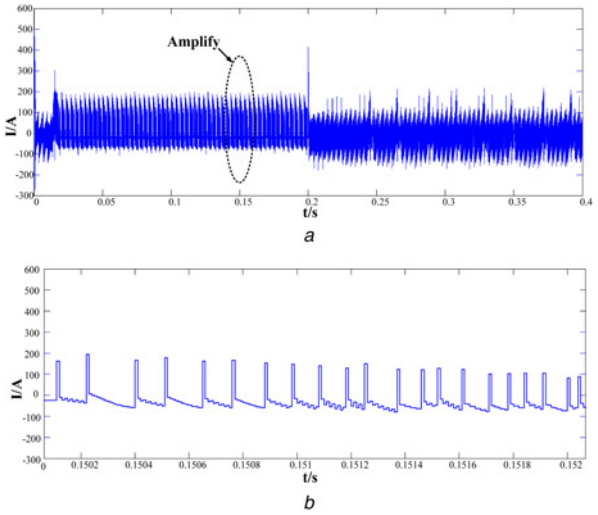

Fig. 15 *Current of transformer primary side*
a Current of transformer primary side without transformer DC magnetic bias suppression
b Local amplification of current

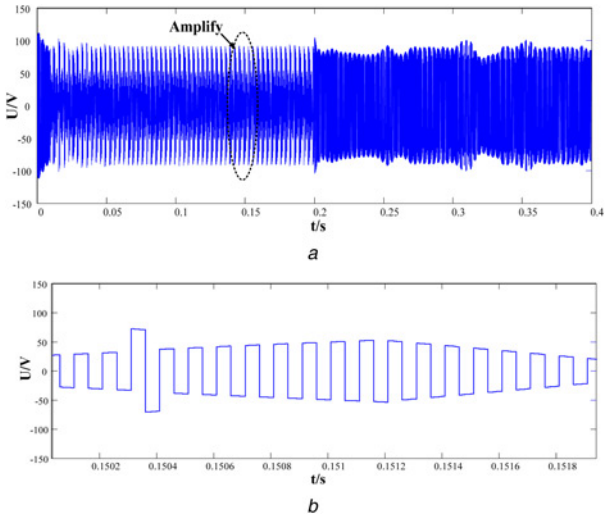

Fig. 16 *Voltage of transformer primary side*
a Voltage of transformer primary side with transformer DC magnetic bias treatment
b Local magnification of voltage

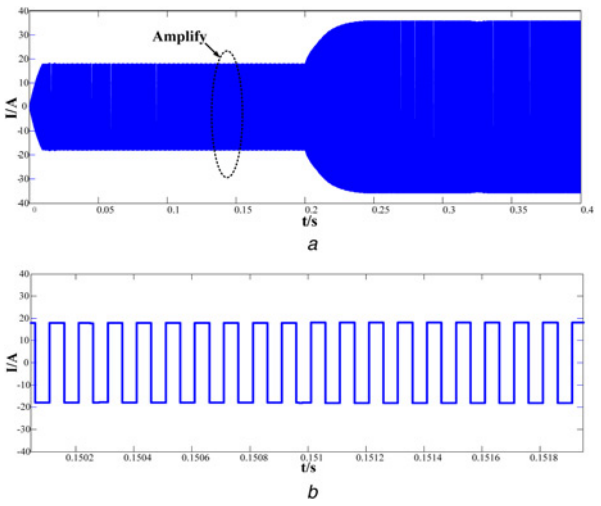

Fig. 17 *Current of transformer primary side*
a Current of transformer primary side with transformer DC magnetic bias treatment
b Local magnification of current

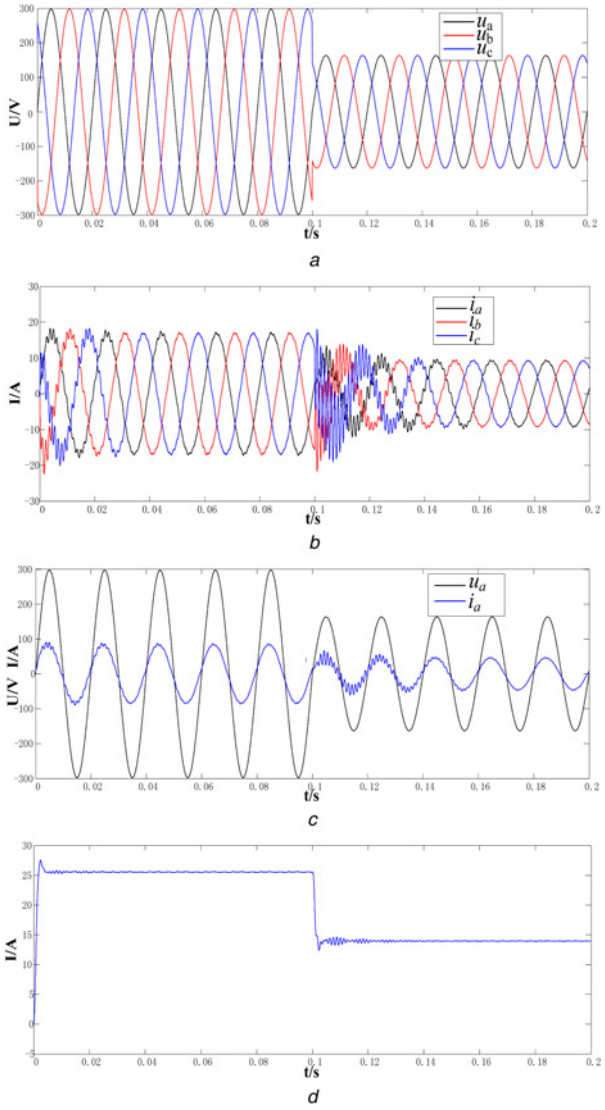

Fig. 18 *Diagrams of input voltage felled based on B-C-SVM*
a Input voltages
b Input currents
c Voltage and current of *A* phase
d Output current

of abnormal input voltage. This is what the existing modulation strategy cannot do.

2.2.5 Distributing pulse sequence considering transformer DC magnetic bias: There is a problem of DC magnetic bias in transformer for RMC topology due to uncertain random switching sequence in conventional MPC; thus, the pulse sequence in MPC had to be re-distributed to suppress the transformer magnetic bias [17, 18].

In a switch period Ts, the optimal switching states selected in a conventional MPC with uncertain random switching sequence are V_1 and V_2, then the diagram of the RMC rectifier stage output voltage sequence is shown in Fig. 9*a*. There are all positive voltage in transformer primary under this switch state selection method, which would cause the problem of transformer DC magnetic bias.

It can be seen in Table 1 that there are two opposite output voltage using different pulse sequence in RMC rectifier stage, such as output voltage U_{ab} in DC-link by using first pulse sequence (V_1) is opposite to the output voltage U_{ba} by using fourth pulse sequence (V_4) in Table 1, output voltage U_{ac} by using second pulse sequence (V_2) is opposite to the output voltage U_{ca} by using fifth pulse sequence (V_5). Thus, one cycle can be split to two equal cycles. At the first equal cycle (Ts/2), the switching state (V_1 and V_2) used is the optimal switching state selected by MPC without transformer DC magnetic bias suppression. At the next equal cycle (Ts/2), the switching state (V_4 and V_5) used is opposite to optimal switching state (V_1 and V_2) as we can see in Table 1. So, the two adjacent pulse sequences are distributed according to the two opposite output voltage such as U_{ab} and U_{ba}, U_{ac} and U_{ca} as shown in Fig. 9*b*. The equivalent circuit is shown in Fig. 10.

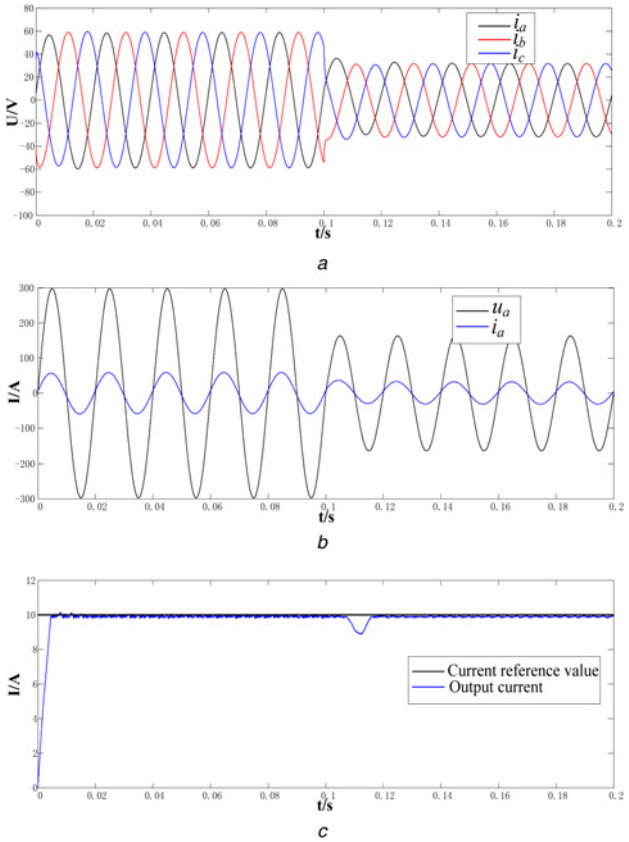

Fig. 19 *Diagrams of input voltage felled based on MPC*
a Input currents
b Voltage and current of *A* phase
c Output current

Through this method of pulse sequence distributing, the transformer magnetic bias in RMC topology can be effectively solved.

3 Results

Simulation are performed by using MATLAB R2010b/Simulink to validate the proposed method. Fig. 11 shows the simulation model of the proposed control method of MPC for RMC. Table 4 shows the simulation parameter.

Fig. 12 shows the input phase voltage and current. It can be seen that the input phase current is in phase with input voltage resulting in high power factor. Fig. 13 shows the output current and its reference. Seen from Fig. 13, the output currents follow the reference value with high accuracy. Moreover, it can also maintain good dynamic performance when the current suddenly increases.

Figs. 14 and 15 show voltage and current of transformer primary side by using conventional MPC in RMC without transformer DC magnetic bias suppression. It can be seen that the voltage and current are disorganised. This will lead to a problem of DC

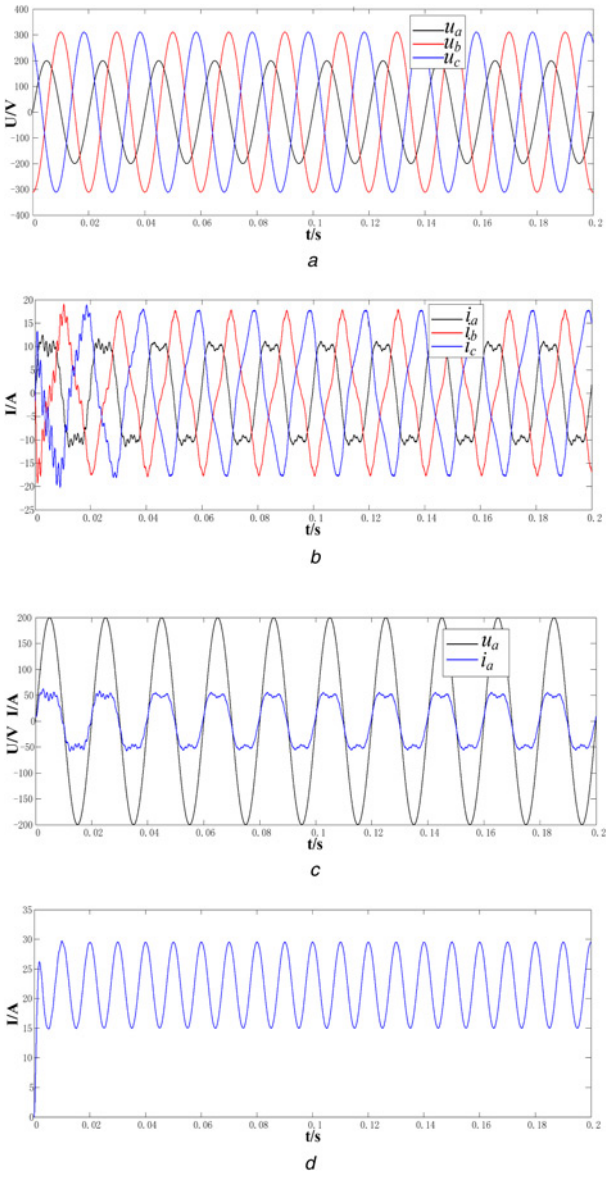

Fig. 20 *Diagrams of an unbalanced three-phase voltage based on B-C-SVM*
a Input voltages
b Input currents
c Voltage and current of *A* phase
d Output current

doi: 10.1049/joe.2018.0036

magnetic bias in transformer for RMC topology using a conventional MPC.

Figs. 16 and 17 show voltage and current of transformer primary side by using the proposed MPC with transformer DC magnetic bias suppression. It can be found that voltage and current show a positive or negative state. So, the transformer magnetic bias has been effectively eliminated. The proposed control strategy is verified, too.

To further verify to be immune to abnormal input voltage of the proposed method, the input voltage sag and unbalance are tested for MPC and B-C-SVM in an RMC.

As shown in Fig. 18*a*, the three-phase input voltages decrease to 50% normal value at 0.1 s. Seen from Figs. 18–20, the system with MPC is unit power factor and the output current follow the reference without error even though there is input voltage sag; however, there output current decrease caused by input voltage in a B-C-SVM system.

An unbalanced three-phase input voltage $U_s = [150\ \sin(100\pi t)\ 311\ \sin(100\pi t - 90°)\ 311\ \sin(100\pi t + 120°)]$ shown in Fig. 21*a* was used to test the performance of B-C-SVM and MPC for RMC. Seen from Fig. 21, under B-C-SVM, the input currents have lost its sinusoidal characteristic, there is serious fluctuation in the output current caused by unbalanced input voltage. Seen from Fig. 21, the system with MPC is in unit power factor and output current follow with reference even though there is an unbalanced set of input voltage.

Comparing with the input and output characteristics of RMC controlled by MPC and B-C-SVM under abnormal operating conditions, it is shown that the MPC in an RMC system present to be strong immune to abnormal input voltage than B-C-SVM.

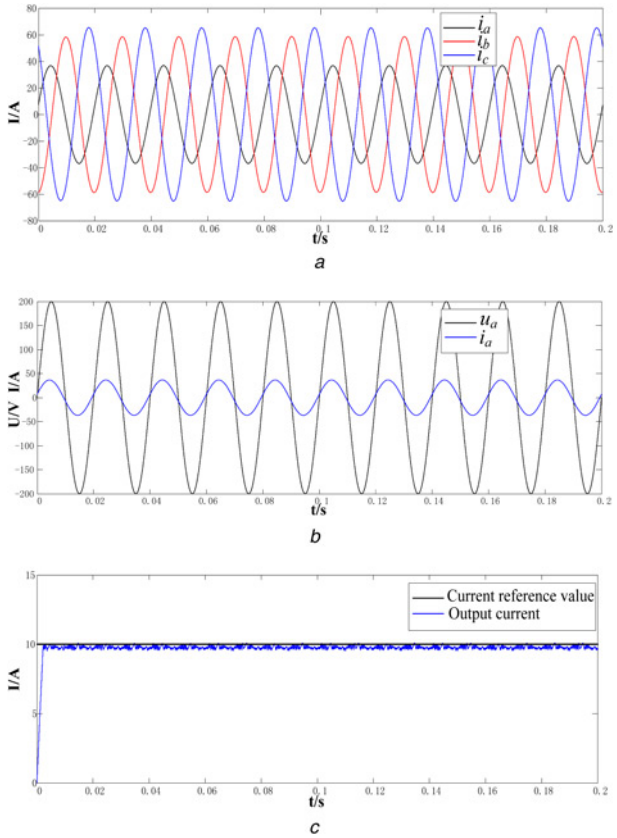

Fig. 21 *Diagrams of an unbalanced three-phase voltage based on MPC*
a Input currents
b Voltage and current of *A* phase
c Output current

4 Conclusion

An effective method of MPC considering transformer DC magnetic bias for an RMC has been proposed in this paper. The control scheme selects the switching state that minimises the error in the output current and input instantaneous reactive according to their reference values; meanwhile, the pulse sequence in MPC has been re-distributed to suppress the DC magnetic bias in transformer for RMC; thus, the transformer magnetic bias has been effectively eliminated without extra control circuit. Moreover, MPC also presents stronger immunity to the influence of abnormal input voltage than B-C-SVM. The system owns a good performance in terms of input power factor and output current tracking using the proposed method. The feasibility and validity of the proposed control scheme in an RMC has been verified by simulation results.

5 Acknowledgments

Project supported by National Natural Science Foundation of China (51307138); State Key Laboratory of Large Electric Drive System and Equipment Technology (SKLLDJ022016008); Research Funding for Xi'an University of Technology (2016CX034); Shaanxi international exchange and cooperation project (2017KW-035).

6 References

[1] Garces A., Molinas M.: 'Reduced matrix converter operated as current source for off-shore wind farms'. 2010 14th Int. Power Electronics and Motion Control Conf., 2010, pp. 149–154
[2] Garces A., Molinas M.: 'A study of efficiency in a reduced matrix converter for offshore wind farms', *IEEE Trans. Ind. Electron.*, 2012, **59**, (1), pp. 184–193
[3] Deng W.-L., Long M.-Z., Cui G.-P.: 'Bipolar space vector pulse-width modulation of high frequency link two-stage matrix converter', *Electr. Mach. Control*, 2013, **17**, (11), pp. 75–82
[4] Zhou Y., Song W.Z., Yan H.: 'Research on bipolar space vector pulse-width modulation strategy for reduced matrix converter', *Power Supply Technol. Appl.*, 2016, 5, pp. 15–19
[5] Krishnamoorthy H.S., Garg P., Enjeti P.N.: 'A matrix converter-based topology for high power electric vehicle battery charging and V2G application'. 2012 Conf. on IEEE Industrial Electronics Society (IECON), 2012, vol. 2, pp. 2866–2871
[6] Rodriguez J., Cortes P., Kennel R., *ET AL.*: 'Model predictive control – a simple and powerful method to control power converters'. Power Electronics and Motion Control Conf., 2009, pp. 41–49
[7] Yaramasu V., Rivera M., Narimani M., *ET AL.*: 'Model predictive approach for a simple and effective load voltage control of four-leg inverter with an output, filter', *IEEE Trans. Ind. Electron.*, 2014, **61**, (10), pp. 5259–5270
[8] Zhang Y., Peng Y., Qu C.: 'Model predictive control and direct power control for PWM rectifiers with active power ripple minimization', *IEEE Trans. Ind. Appl.*, 2016, **52**, (6), pp. 4909–4918
[9] Correa P., Rodriguez J., Rivera M., *ET AL.*: 'Predictive control of an indirect matrix converter', *IEEE Trans. Ind. Electron.*, 2008, **56**, (6), pp. 1847–1853
[10] Kolar J.W., Friedli T., Krismer F., *ET AL.*: 'The essence of three-phase AC–AC converter system'. Proc. 13th Power Electron Motion Control Conf., Poznan, Poland, September 2008, pp. 27–42
[11] Song W., Zhong Y., Zhang H., *ET AL.*: 'A study of Z-source dual-bridge matrix converter immune to abnormal input voltage disturbance and with high voltage transfer ratio', *IEEE Trans. Ind. Inf.*, 2013, **9**, (2), pp. 828–838
[12] Ping X., Jing B.: 'PCHD control strategy of three phase current type PWM rectifier'. 29th Chinese Control and Decision Conf. (CCDC), 2017, pp. 7057–7061
[13] Liu Y., Liu Y., Abu-Rub H., *ET AL.*: 'Model predictive control of matrix converter based solid state transformer'. IEEE Int. Conf. on Industrial Technology, 2016, pp. 1248–1253
[14] Correa P., Rodríguez J., Rivera M., *ET AL.*: 'Predictive control of an indirect matrix converter'. *IEEE Trans. Ind. Electron*, 2009, **56**, (6), pp. 1847–1852

[15] Vargas R., Rodríguez J., Rojas C.A., *ET AL.*: 'Predictive control of an induction machine fed by a matrix converter with increased efficiency and reduced common-mode voltage'. *IEEE Trans. Energy Convers.*, 2014, **29**, (2), pp. 473–485
[16] Cortes P., Kouro S., La Rocca B., *ET AL.*: 'Guidelines for weighting factors design in model predictive control of power converters and drives'. IEEE Int. Conf. on Industrial Technology, 2009, pp. 1–7
[17] Bai B., Chen Z., Chen D., *ET AL.*: 'DC bias elimination and integrated magnetic technology in power transformer', *IEEE Trans. Magn.*, 2015, **51**, (11), pp. 1–1
[18] Enshu J., Kuiying Y., Fangsen C.: 'Effects of DC magnetic bias on differential protection of transformer'. 2011 Int. Conf. on Advanced Power System Automation and Protection (APAP), Beijing, China, 2011, vol. 3, pp. 2182–2186